

Survival probability for high mass diffraction

E.Gotsman ^{*} , A. Kormilitzin[†] , E. Levin [‡] and U. Maor [§]

*Department of Particle Physics, School of Physics and Astronomy
 Raymond and Beverly Sackler Faculty of Exact Science
 Tel Aviv University, Tel Aviv, 69978, Israel*

ABSTRACT: In this paper the values of survival probabilities of the large rapidity gaps are found for high mass diffraction in proton-proton collisions, and in deep inelastic scattering. We show that these values are very sensitive to the experimental information on the cross section of the double diffraction production. We confirm the idea of Ref. [1], that the measurement of high mass diffraction in deep inelastic scattering, will allow us to extract information on both the value of the survival probability, and on the value of the triple Pomeron vertex.

KEYWORDS: Soft Pomeron,BFKL Pomeron, Diffractive cross sections, Survival probability .

PACS: 13.85-*t*, 13.85.*Hd*, 11.55.-*m*, 11.55.*Bq*

^{*}Email: gotsman@post.tau.ac.il;

[†]Email:andreyk1@post.tau.ac.il

[‡]Email: leving@post.tau.ac.il, levin@mail.desy.de;

[§]Email:maor@post.tau.ac.il;

Contents

1. Introduction	1
2. Survival probability for triple Pomeron vertex in proton-proton collisions.	5
2.1 Survival probability in the eikonal model	5
2.2 Two channel model: main ideas and formulae	6
2.3 Final formula	7
2.4 Survival probability and the total cross section for diffractive production	7
2.5 Two models for fitting the experimental data	8
2.5.1 Model A:	8
2.5.2 Model B:	9
2.6 Results of calculation	9
3. Survival probability for triple Pomeron vertex for J/Ψ-proton collisions.	11
4. Conclusions	15

1. Introduction

A large rapidity gap (LRG) process is defined as one where no hadrons are produced in a sufficiently large rapidity region. Diffractive LRG are assumed to be produced by the exchange of a colour singlet object with quantum numbers of the vacuum, which we will refer to as the Pomeron. We wish to estimate the probability that LRG, which occur in diffractive events containing a hard sub process, survive rescattering effects i.e. survive the population of the gaps by secondary particles coming from the underlying event.

At high energies, elastic and inelastic diffractive processes account for about 40% of the total $pp(\bar{p}p)$ cross section.

We would like to remind the reader that:-

1. The small t behaviour of the scattering amplitude originates mostly from large impact parameter b values.

2. The region associated with large b , where the optical density (i.e. opacity) $\Omega(b)$ becomes small provides the major contribution to the survival probability $\langle |S|^2 \rangle$ of the large rapidity gaps. Consequently, $\langle |S|^2 \rangle$ decreases with increasing energy due to the growth of the opacity of the interaction.
3. $\langle |S|^2 \rangle$ is not only dependent on the probability of the initial state to survive, but is sensitive to the spatial distribution of the partons inside the incoming hadrons, and thus, on the dynamics of the whole diffractive part of the scattering matrix.
4. $\langle |S|^2 \rangle$ is not universal. It depends on the particular hard subprocess, as well as the kinematic configurations. It also depends on the nature of the colour singlet (P, W/Z or photon) exchange which is responsible for the LRG.

Historically, both Dokshitzer et al. [6] and Bjorken [7], suggested utilizing LRG as a signature for Higgs production in a through a W-W fusion sub process, in hadron-hadron collisions. It turns out that the LRG processes give a unique opportunity to measure the high energy asymptotic behaviour of the amplitudes at short distances, where one can use methods developed for perturbative QCD (pQCD) to calculate the amplitudes. Considering a typical LRG process - the production of two jets with large transverse momenta $\vec{p}_{t1} \approx -\vec{p}_{t2} \gg \mu$, with LRG between the two jets. μ is a typical mass scale of the soft interactions.

$$\begin{aligned} p(1) + p(2) &\longrightarrow M_1[\text{hadrons} + \text{jet}_1(y_1, p_{t1})] \\ &+ \text{LRG}[\Delta y = |y_1 - y_2|] + M_2[\text{hadrons} + \text{jet}_2(y_2, p_{t2})] \end{aligned} \quad (1.1)$$

where y_1 and y_2 are the rapidities of the jets and $\Delta y = |y_1 - y_2| \gg 1$. The production of two jets with LRG between them can occur because:

1. A fluctuation in the rapidity distribution of a typical inelastic event. However, the probability for such a fluctuation is proportional to $e^{-\frac{\Delta y}{L}}$, where L denotes the value of the correlation length. We can evaluate $L \approx \frac{1}{\frac{dn}{dy}}$, where $\frac{dn}{dy}$ is the number of particles per unit in rapidity. Rough estimates using the Tevatron data shows that $L \approx 0.5 - 1$. A LRG means that $\Delta y \gg L$, and consequently the probability is small;
2. The exchange of a colourless state in QCD. This exchange is given by the amplitude of the high energy interaction at short distances, which we call the hard Pomeron exchange. We define F_s to be the ratio between the cross section due to the above Pomeron exchange, and the typical inelastic event cross section generated by gluon exchange. In QCD we do not expect this ratio to decrease as a function of the rapidity gap $\Delta y = y_1 - y_2$. For a BFKL Pomeron [8], we expect an increase once $\Delta y \gg 1$. Using a simple QCD model for the Pomeron , in which it is approximated by two gluon exchange [9], Bjorken [7] gave the first estimate for $F_s \approx 0.15$, which is unexpectedly large.

As noted by Bjorken, [7] and GLM [11], we are not able to measure F_s directly in a LRG experiment. The experimentally measured ratio of the number of events with a LRG, to the number of events without a

LRG is not equal to F_s , but has to be modified by an extra factor which we call the survival probability of LRG.

$$f_{gap} = \langle |S|^2 \rangle \times F_s . \quad (1.2)$$

The appearance of $\langle |S|^2 \rangle$ in Eq. (1.2) has a very simple physical interpretation. It is the probability that the LRG due to Pomeron exchange, will not be filled by the produced particles (partons and/or hadrons) from the rescattering of spectator partons , or from the emission of bremsstrahlung gluons from partons taking part in the hard interaction, or from the hard Pomeron.

$$\langle |S|^2 \rangle = \langle |S_{\text{bremsstrahlung}}(\Delta y = |y_1 - y_2|)|^2 \rangle \times \langle |S_{\text{spectator}}(s)|^2 \rangle , \quad (1.3)$$

where s denotes the total c.m. energy squared.

- $\langle |S_{\text{bremsstrahlung}}(\Delta y)|^2 \rangle$ can be calculated in pQCD [10], it depends on the kinematics of each specific process, and on the value of the LRG .
- To calculate $\langle |S_{\text{spectator}}(s)|^2 \rangle$ we need to find the probability that all partons with rapidity $y_i > y_1$ in the first hadron, and all partons with $y_j < y_2$ in the second hadron, do not interact inelastically and, hence, do not produce additional hadrons in the LRG. This is a difficult problem, since not only partons at short distances contribute to such a calculation, but also partons at long distances for which the pQCD approach is not valid. Many attempts have been made to estimate $\langle |S_{\text{spectator}}(s)|^2 \rangle$ [7] [11] [12] [13] [14] [15] [16], but a unique solution has, still not been found.

An obvious check is to compare the calculated values of $\langle |S_{\text{spectator}}(s)|^2 \rangle$ obtained in different models for different reactions. The Durham group [1] suggested a very interesting check, proposing to extract the 3 Pomeron vertex coupling (G_{3P}) utilizing the measurement of large mass diffraction dissociation in the reaction

$$\gamma^*(Q^2, x_{Bj}) + p \implies J/\Psi + [\text{LRG}] + X(M^2 \gg m_p) \quad (1.4)$$

The cross section of the process can be described by the Mueller diagram (see Fig. 1). Which is initiated by the charm component of the photon which has a small absorptive cross section since its interaction stems from short distances ($r \propto 1/m_c$ where m_c is the mass of charm quark). Thus, the probability for additional rescatterings (Fig. 2) is relatively small resulting in a high survival probability. This is to be compared with the corresponding high mass diffraction in an hadronic pp ($\bar{p}\bar{p}$ reaction (Fig. 3), for which we expect the rescatterings (Fig. 4) to be significant, resulting in a small survival probability. It is therefore very probable, that present extractions [3] of the $3P$ coupling are underestimated. Comparing the values of G_{3P} obtained in the above two channels, taking into account their (different) survival probabilities, leads to a more reliable measure of the $3P$ coupling, and provides a check of the various theoretical estimates of the survival probabilities.

In this paper, we address two main topics: the value of the survival probability for triple Pomeron vertex in proton-proton collisions, and the calculation of the survival probability for the reaction of Eq. (1.4). In

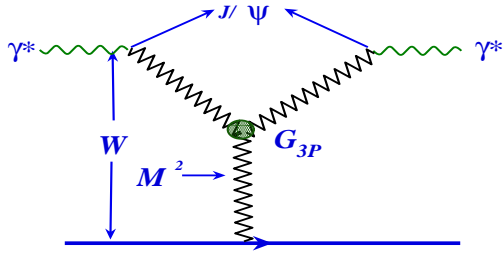


Figure 1: The general diagram for diffraction production of large masses in γ^* - proton collisions at high energy. The zigzag line denotes the soft Pomeron.

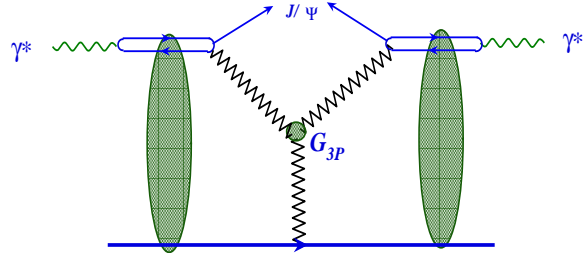


Figure 2: The general diagram for calculating the survival probability for diffraction production of large masses in γ^* -proton collisions at high energy. The zigzag line denotes the soft Pomeron.

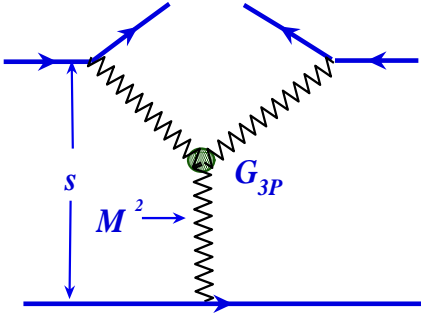


Figure 3: The general diagram for diffraction production of large masses in proton-proton collisions at high energy. The zigzag line denotes the soft Pomeron.

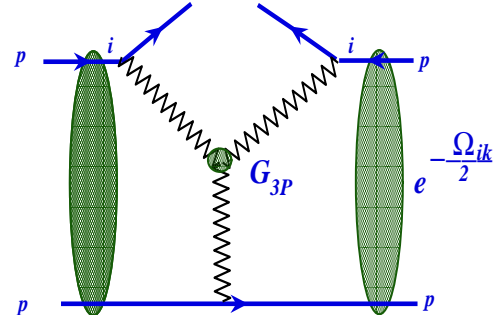


Figure 4: The general diagram for calculating the survival probability for diffraction production of large masses in proton-proton collisions at high energy. The zigzag line denotes the soft Pomeron.

the next section we calculate $\langle |S_{\text{spectator}}(s)|^2 \rangle$ for high mass diffraction in proton-proton scattering in a three channel model for the soft interaction (see Refs. [5]). The survival probability turns out to be rather small, and in an agreement with the estimates of Ref. [1]. In section 3 we present our estimates for the survival probability of the process of Eq. (1.4). These calculations show that we have to take into account the values of $\langle |S_{\text{spectator}}(s)|^2 \rangle$. However, the reliability and accuracy of the theoretical estimates are much better than in the proton-proton case. Hence, we consider the experimental ratio

$$R = \frac{\sigma_{\text{diff}}(pp \rightarrow p + M(M \gg m))}{\sigma_{\text{diff}}(\gamma^* p \rightarrow J/\Psi + M(M \gg m))} \quad (1.5)$$

as a check of our procedure for survival probability calculations. In the conclusions, we discuss the main results and unsolved problems.

2. Survival probability for triple Pomeron vertex in proton-proton collisions.

2.1 Survival probability in the eikonal model

The cross section for diffractive dissociation in the region of large M can be viewed as the Mueller diagram of Fig. 3, which can be rewritten in terms of the triple Pomeron vertex (see Refs. [?]), namely,

$$M^2 \frac{d\sigma^{SD}}{dt dM^2} = \frac{g_p^2(t) g_p(q^2 = 0) G_{3P}(t)}{16\pi^2} \left(\frac{s}{M^2}\right)^{2\alpha_P(t)-2} \left(\frac{M^2}{s_0}\right)^{\alpha_P(q^2=0)-1} \quad (2.1)$$

where $g(t)$ describe the vertex of Pomeron - proton interaction, and G_{3P} stands for the triple Pomeron vertex. However, this diagram does not take into account the possibility of additional rescatterings of interacting particles shown in Fig. 4. The result can be written in the following form

$$M^2 \frac{d\sigma^{SD}}{dt dM^2} = S_{SD}^2 \frac{g_p^2(t) g_p(q^2 = 0) G_{3P}(t)}{16\pi^2} \left(\frac{s}{M^2}\right)^{2\alpha_P(t)-2} \left(\frac{M^2}{s_0}\right)^{\alpha_P(q^2=0)-1} \quad (2.2)$$

The factor S_{SD}^2 ¹ is defined as

$$S_{SD}^2 = \frac{\int d^2 k_t M^2 \frac{d\sigma^{SD}}{dk_t^2 dM^2} (\text{Fig. 4})}{\int d^2 k_t M^2 \frac{d\sigma^{SD}}{dk_t^2 dM^2} (\text{Fig. 3})} \quad \text{with } t = -k_t^2 \quad (2.3)$$

The easiest way to calculate the diagram of Fig. 4 is to switch to the impact parameter for the representation of the diagram of Fig. 3. We can do this by introducing the momentum q along the lowest pomeron in Fig. 3. In this case

$$T(S, M^2; q) \equiv \int d^2 k_t M^2 \frac{d\sigma^{SD}}{dk_t^2 dM^2} (\text{Fig. 3}) \longrightarrow \int d^2 k_t \frac{g_p(k_t^2) g_p((\vec{k} - \vec{q})_t^2) g_p(q_t^2) G_{3P}(k_t^2, (\vec{k} - \vec{q})_t^2, q^2)}{16\pi^2} \left(\frac{s}{M^2}\right)^{\alpha_P(k_t^2) + \alpha_P((\vec{k} - \vec{q})_t^2) - 2} \left(\frac{M^2}{s_0}\right)^{\alpha_P(q^2)-1} \quad (2.4)$$

From Eq. (2.4) we find the form of this amplitude in impact parameter space

$$T(S, M^2; b) \equiv \int \frac{d^2 q}{(2\pi)^2} A(S, M^2; q) \quad (2.5)$$

Using a linear approximation for the Pomeron trajectory and a Gaussian form for all vertices, namely,

$$\alpha_P(t) = 1 + \Delta \alpha'_P t; \quad g_p(k^2) = g_p(0) e^{-b_p k^2}; \quad G_{3P}(k_1, k_2, k_3) = G_{3P}(0, 0, 0) e^{-b_p (k_1^2 + k_2^2 + k_3^2)}; \quad (2.6)$$

we find that

$$T(S, M^2; b) = \frac{g_{3P}}{16\pi^2} \nu(\xi) \nu(\xi) \nu(y) \frac{\pi}{d(\xi) + d(\xi) + d(y)} \exp\left(-\frac{d(y) [d(\xi) + d(\xi)]}{d(\xi) + d(\xi) + d(y)} b^2\right) \quad (2.7)$$

¹ S_{SD}^2 denotes the SD survival probability, and is the same factor that we as $\langle |S_{\text{spectator}}(s)|^2 \rangle$ for the specific reaction.

where

$$y = \ln(M^2/s_0); \quad \xi = \ln(s/M^2); \quad g_{3P} \equiv G_{3p}(0,0,0)/g_p(0); \quad (2.8)$$

$$\nu(y) = \frac{g_p^2(0)}{\pi \bar{R}^2(y)} e^{\Delta y}; \text{ with } \bar{R}^2(y) = 2R_0^2 + 2r_0^2 + 4\alpha'_P y \text{ and } d(y) \equiv \frac{1}{\bar{R}^2(y)}; \quad (2.9)$$

Using Eq. (2.7) the expression for the survival probability (see Eq. (2.3)) in the simple eikonal model for rescattering corrections, can be written as:

$$S_{SD}^2 = \frac{\int d^2b T(s, M^2; b) \exp(-\Omega(\xi + y; b))}{\int d^2b T(s, M^2; b)} \quad \text{where } \Omega(\xi + y; b) = \nu_{pp} e^{-\frac{b^2}{R_{pp}(\xi + y)}} \quad (2.10)$$

where

$$\text{with } \nu_{pp} = \frac{g_p^2(0)}{\pi R_{pp}(\xi + y)} e^{\Delta(\xi + y)} \text{ and } R_{pp}(\xi + y) = 4R_{0,p}^2 + 4\alpha'_P(\xi + y); \quad (2.11)$$

2.2 Two channel model: main ideas and formulae

In the eikonal model only the elastic rescatterings have been taken into account. The two channel model has been developed so as to also include rescatterings through diffractive dissociation (see Refs. [?, 5] and references therein). In the two channel model the diffractively produced hadrons are considered as a single hadronic state which is described by the wave function Ψ_D which is orthogonal to the wave function Ψ_h of the hadron (proton in the case of interest), $\langle \Psi_h | \Psi_D \rangle = 0$.

Introducing two wave functions that diagonalize the interaction matrix \mathbf{T}

$$A_{i,k} = \langle \Psi_i | \Psi_k | \mathbf{T} | P s_i | \Psi_{k'} \rangle = A_{i,k} \delta_{i,i'} \delta_{k,k'} \quad (2.12)$$

we can rewrite the amplitude $A_{i,k}$ in the form that satisfies the unitarity constraints

$$A_{i,k}(s, b) = i \left(1 - \exp \left(-\frac{\Omega_{i,k}(s, b)}{2} \right) \right); \quad G_{i,k}^{in}(s, b) = 1 - \exp(-\Omega_{i,k}(s, b)) \quad (2.13)$$

G^{in} is the probability for all inelastic interactions in the scattering of particle i off particle k . From Eq. (2.13), the probability that none of the inelastic interactions occur is equal to $\exp(-\Omega_{i,k}(s, b))$.

In this representation the observed states can be written in the form

$$\Psi_h = \alpha \Psi_1 + \beta \Psi_2; \quad \Psi_D = -\beta \Psi_1 + \alpha \Psi_2; \quad \text{with } \alpha^2 + \beta^2 = 1 \quad (2.14)$$

The obvious generalization of Eq. (2.7) is

$$T(s, M^2; b) = \sum_{i,k,l} \langle p | l \rangle^2 \langle p | k \rangle T_k^{l,i}(s, M^2; b) \langle p | k \rangle \langle p | i \rangle^2 \quad (2.15)$$

where $\langle p | 1 \rangle = \alpha$ and $\langle p | 2 \rangle = \beta$

$$T_k^{l,i}(S, M^2; b) = \frac{g_{3P}}{16\pi^2} \nu_l(\xi) \nu_i(\xi) \nu_k(y) \frac{\pi}{d_l(\xi) + d_i(\xi) + d_k(y)} \exp \left(-\frac{d_k(y) [d_l(\xi) + d_i(\xi)]}{d_l(\xi) + d_i(\xi) + d_k(y)} b^2 \right) \quad (2.16)$$

where $g_{3P} = G_{3P}/g_1(0)$ and

$$\nu_k(y) = \frac{g_k(0)g_1(0)}{\pi \bar{R}_k^2(y)} e^{\Delta y} ; \text{ with } \bar{R}_k^2(y) = 2R_{0,k}^2 + 2r_0^2 + 4\alpha'_P y \text{ and } d_k(y) \equiv \frac{1}{\bar{R}_k^2(y)}; \quad (2.17)$$

The numerator of Eq. (2.10) is

$$\begin{aligned} & \int d^2 k_t M^2 \frac{d\sigma^{SD}}{d k_t^2 dM^2} (Fig. 4) = \\ & \int d^2 b \sum_{i,k,l} \langle p|l \rangle^2 \langle p|k \rangle e^{-\frac{\Omega_{l,k}(s,b)}{2}} T_k^{l,i}(s, M^2; b) e^{-\frac{\Omega_{i,k}(s,b)}{2}} \langle p|k \rangle \langle p|i \rangle^2 \end{aligned} \quad (2.18)$$

For $\Omega_{i,k}(s, b)$ we take

$$\Omega_{i,k}(s, b) = \nu_{i,k} e^{-\frac{b^2}{R_{i,k}^2(\xi+y)}} \quad (2.19)$$

where

$$\text{where } \nu_{i,k} = \frac{g_i(0)g_k(0)}{\pi R_{i,k}^2(\xi+y)} \left(\frac{s}{s_0} \right)^\Delta \text{ with } R_{i,k}^2(\xi+y) = 2R_{0,i}^2 + 2R_{0,k}^2 + 4\alpha'_P(\xi+y). \quad (2.20)$$

2.3 Final formula

The survival probability can be calculated as the ratio

$$S_{3P}^2 = \frac{\int d^2 b N(\xi, y; b)}{\int d^2 b D(\xi, y; b)} \quad (2.21)$$

$$\begin{aligned} N(\xi, y; b) = & \alpha^6 T_1^{1,1}(b) e^{-\Omega_{1,1}(b)} + 2\alpha^4 \beta^2 T_1^{1,2}(b) e^{-\frac{\Omega_{1,1}(b)+\Omega_{1,2}(b)}{2}} + \alpha^2 \beta^4 T_1^{2,2}(b) e^{-\Omega_{1,2}(b)} \\ & + \alpha^4 \beta^2 T_2^{1,1}(b) e^{-\Omega_{1,2}(b)} + 2\alpha^2 \beta^4 T_2^{1,2}(b) e^{-\frac{\Omega_{2,2}(b)+\Omega_{1,2}(b)}{2}} + \beta^6 T_2^{2,2}(b) e^{-\Omega_{2,2}(b)} \end{aligned} \quad (2.22)$$

$$\begin{aligned} D(\xi, y; b) = & \alpha^6 T_1^{1,1}(b) + 2\alpha^4 \beta^2 T_1^{1,2}(b) + \alpha^2 \beta^4 T_1^{2,2}(b) \\ & + \alpha^4 \beta^2 T_2^{1,1}(b) + 2\alpha^2 \beta^4 T_2^{1,2}(b) + \beta^6 T_2^{2,2}(b) \end{aligned} \quad (2.23)$$

2.4 Survival probability and the total cross section for diffractive production

For completeness of presentation we calculate the integrated cross section of diffractive dissociation in the two channel model, together with the elastic and total cross section. The amplitude for elastic scattering and for the diffractive production have the following form (see Ref. [5])

$$a_{el}(s; b) = i \left(1 - \alpha^2 e^{-\frac{\Omega_{1,1}(s,b)}{2}} + 2\alpha^2 \beta^2 e^{-\frac{\Omega_{1,2}(s,b)}{2}} + \beta^4 e^{-\frac{\Omega_{2,2}(s,b)}{2}} \right); \quad (2.24)$$

$$a_{sd}(s; b) = i \alpha \beta \left(-\alpha^2 e^{-\frac{\Omega_{1,1}(s,b)}{2}} + (\alpha^2 - \beta^2) e^{-\frac{\Omega_{1,2}(s,b)}{2}} + \beta^2 e^{-\frac{\Omega_{2,2}(s,b)}{2}} \right); \quad (2.25)$$

$$a_{dd}(s; b) = i \alpha^2 \beta^2 \left(e^{-\frac{\Omega_{1,1}(s,b)}{2}} - 2 e^{-\frac{\Omega_{1,2}(s,b)}{2}} + e^{-\frac{\Omega_{2,2}(s,b)}{2}} \right); \quad (2.26)$$

Using Eq. (2.19) and Eq. (2.20) as well as the general formulae for the cross section, namely,

$$\sigma_{tot}(s) = 2 \int d^2 b |a_{el}(s; b)|^2; \quad \sigma_{el}(s) = \int d^2 b |a_{el}(s; b)|^2; \quad (2.27)$$

$$\sigma_{sd}(s) = \int d^2 b |a_{sd}(s; b)|^2; \quad \sigma_{dd}(s) = \int d^2 b |a_{dd}(s; b)|^2;$$

It is instructive to present the calculation for diffractive production in the form of a survival probability (see Fig. 5), which we define as the ratio of the output corrected cross section and the input non corrected diffractive production cross section.

$$S_{sd}^2 = \frac{\int d^2 b |a_{sd}(s, b)|^2}{\int d^2 b |a_{sd}^1(s, b)|^2}; \quad (2.28)$$

where $a_{sd}(s; b) = \frac{i\alpha\beta}{2} (-\alpha^2 \Omega_{1,1}(s, b) + (\alpha^2 - \beta^2) \Omega_{1,2}(s, b) + \beta^2 \Omega_{2,2}(s, b))$

We will discuss the result and interpretation of calculations in the next subsection.

2.5 Two models for fitting the experimental data

The calculation of survival probabilities requires a specification of the opacities $\Omega_{i,k}(s, b)$. These are based on a global fit of the experimental soft scattering data. To this end we have constructed two models based on the general formulae given in Eq. (2.16) - Eq. (2.20), but with different input assumptions.

2.5.1 Model A:

In this model we assume that the double diffraction is negligible, and so take a_{dd} in Eq. (2.26) to be zero. This equation allows us to express $\Omega_{2,2}$ in terms of $\Omega_{1,1}$ and $\Omega_{1,2}$, leading to the following formulae (see Refs. [?, ?]):

$$a_{el}(s, b) = i \left(1 - \exp \left(-\frac{\Omega_1(s, b)}{2} \right) - 2\beta^2 \exp \left(-\frac{\Omega_1(s, b)}{2} \right) \left(1 - \exp \left(-\frac{\Delta\Omega(s, b)}{2} \right) \right) \right); \quad (2.29)$$

$$a_{sd}(s, b) = -i\alpha\beta \exp \left(-\frac{\Delta\Omega(s, b)}{2} \right) \left(1 - \exp \left(-\frac{\Delta\Omega(s, b)}{2} \right) \right); \quad (2.30)$$

$$\text{with } \Delta\Omega = \Omega_2 - -\Omega_1; \Omega_1 \equiv \Omega_{1,1} \text{ and } \Omega_2 \equiv \Omega_{1,2} \quad (2.31)$$

$$\Omega_1(s, b) = \frac{g_1^2}{\pi R_1^2(s)} \left(\frac{s}{s_0} \right)^\Delta \exp \left(-\frac{b^2}{R_1^2(s)} \right); \quad (2.32)$$

$$\Delta\Omega_1(s, b) = \frac{g_2^2}{\pi R_2^2(s)} \left(\frac{s}{s_0} \right)^\Delta \exp \left(-\frac{b^2}{R_2^2(s)} \right); \quad (2.33)$$

Model	Δ	β	$R_{0,11}^2$	$R_{0,12}^2$	$R_{0,22}^2$	r_0^2	α'_P	g_1	g_2
A	0.126	0.464	$16.34 GeV^{-2}$	$0.5R_{0,11}^2$	0	$0.5 GeV^{-2}$	$0.25 GeV^{-2}$	$3.6 GeV^{-1}$	$12.1 GeV^{-1}$
B(1)	0.150	0.767	$21.88 GeV^{-2}$	$0.5R_{0,11}^2$	0	$0.5 GeV^{-2}$	$0.1675 GeV^{-2}$	$2.2 GeV^{-1}$	$63.34 GeV^{-1}$
B(2)	0.150	0.7834	$20.8 GeV^{-2}$	$0.5R_{0,11}^2$	0	$0.5 GeV^{-2}$	$0.204 GeV^{-2}$	$2.01 GeV^{-1}$	$35.24 GeV^{-1}$

Table 1: Fitted parameters for Models A, B(1) and B(2).

In our notation $\Delta\Omega = \Omega_2 - \Omega_1$, $\Omega_1 \equiv \Omega_{1,1}$ and $\Omega_2 \equiv \Omega_{1,2}$. Following Ref. [?], we assume both Ω_1 and $\Delta\Omega$ to be Gaussians in b .

$$\Omega_1(s, b) = \frac{g_1^2}{\pi R_1^2(s)} \left(\frac{s}{s_0} \right)^\Delta \exp \left(-\frac{b^2}{R_1^2(s)} \right), \quad (2.34)$$

$$\Delta\Omega(s, b) = \frac{g_2^2}{\pi R_2^2(s)} \left(\frac{s}{s_0} \right)^\Delta \exp \left(-\frac{b^2}{R_2^2(s)} \right). \quad (2.35)$$

For R_1^2 and R_2^2 we use Eq. (2.20).

2.5.2 Model B:

In this model we do not make any assumptions regarding the value of the double diffraction, which enters in our fit (see more details in Ref. [5]). We use Eq. (2.19) and Eq. (2.20) to parameterize three independent opacities: $\Omega_{1,1}$, $\Omega_{1,2}$ and $\Omega_{2,2}$, all Gaussians in b .

2.6 Results of calculation

The parameters of Model A have been adjusted, at the time, based on a data fit which included the pp and $p\bar{p}$ total cross sections, integrated elastic cross sections, integrated single diffraction cross sections, and the forward slope of the elastic cross section (see Ref. [?]). As stated, our input assumption was that the double diffractive channel is negligibly small. Its fitted parameters are listed in Table 1.

Model B analysis is based on a new fit to the updated data base utilizing the general formulae given in the previous section and in Ref. [5]. The data base includes also the published [?] double diffraction cross sections. The values of Model B adjusted parameters are given, as well, in Table 1. We present two sets of parameters denoted B(1) and B(2). Even though their fitted g_2 values differ significantly, their χ^2 differ by just 10%. One concludes that the existing data on the diffraction cross sections are not sufficient to constraint the value of g_2 .

Model A and B fitted parameters, specified in Table 1, were used to calculate the survival probabilities for two different soft diffraction processes. S_{3P}^2 corresponds to single diffraction dissociation in the high mass region (see Eq. Eq. (2.21)). S_{sd}^2 is the survival probability corresponding to the entire region of the produced diffracted mass (see Eq. Eq. (2.28)). The calculated survival probabilities are presented in Fig. 5 and we note a significant difference between the various output results. Specifically, we note a few qualitative characteristics:

1. The survival probability resulting from Model A are considerably larger than those of Model B. We trace this difference to the observation that g_2 obtained in Model B is a factor 3-5 larger than its value obtained in Model A. This is a direct consequence of model B being less constraint than model A where the double diffractive amplitude is forced to be zero (breaking Regge factorization).
2. The survival probabilities calculated in Model B(1) are consistently larger than the corresponding B(2) output. In the sd sector, the two models predict values of S_{3P}^2 which differ by an order of magnitude. We associate this difference to the difference in the fitted g_2 values in the two models (see Table 1).
3. We note that Model B output is not stable enough, probably as a result of the small number of double diffractive data points in the fitted data base. However, we stress the qualitative conclusion that opening the double diffraction channel in the Model B, crucially changes the survival probability estimates obtained in the Model A. This conclusion is supported by our observation that Model B fit to the data base of Model A (i.e, no double diffractive data points) results in adjusted parameters similar to those presented in Table 1.
4. With the exception of Model A with $W \gtrsim 3000$ GeV, S_{3P}^2 are consistently higher than S_{sd}^2 . We believe that this reflects the difference in the b dependence of the opacity inputs in the 2 and 3 channel models.
5. The magnitude and behaviour of S_{3P}^2 depends strongly on how we treat the double diffractive production. For both models S_{3P}^2 differs greatly from (S^2) obtained for a single gap configuration in a one channel model, where only elastic rescatterings are considered [?]. S_{3P}^2 is about 3 times larger than S^2 , at the Tevatron and LHC energies, while at Cosmic Ray energies it is 10 times larger.

The soft cross section predictions of Model B(1) at high energies are shown in Fig. 6. The output of Model B(2) is very similar. These results should be confronted with the predictions of Model A (Ref. [?]). The two models are compatible, reproducing the ISR-Tevatron soft data base well. The two models slowly develop a difference at very high energies. Model B predicts $\sigma_{tot} = 111$ mb for the LHC energy, while model A yields a value of $\sigma_{tot} = 103$ mb.

The details of our Model A fit can be found in Ref. [?]. We have used data over the complete ISR-Tevatron range, all in all 55 experimental points. In Model B we have added 5 double diffraction points. In both Model A and B we have employed both a Reggeon and a Pomeron trajectory. The characteristics of the Pomeron trajectory (which dominates at higher energies) are given in Table 1. The results of our calculation and the extrapolation to higher energies for the various quantities are shown in Fig. 5. Our best fit B1 has a $\chi^2/(d.o.f)$ of 1.48, while fit B2 has $\chi^2/(d.o.f)$ of 1.57. As in the two channel Model A fit [?], we note that the relatively high χ^2 obtained in Model B originate mostly from the wide spread of the single diffraction data points. We also note that both fits under estimate the measured values of σ_{dd} , by about 50 percent, and contribute 10 units to the total χ^2 for the five data points (see Ref.[18]). As we have already observed, an unexpected result is the great sensitivity of the calculated survival probabilities to the values of the parameters in the different models.

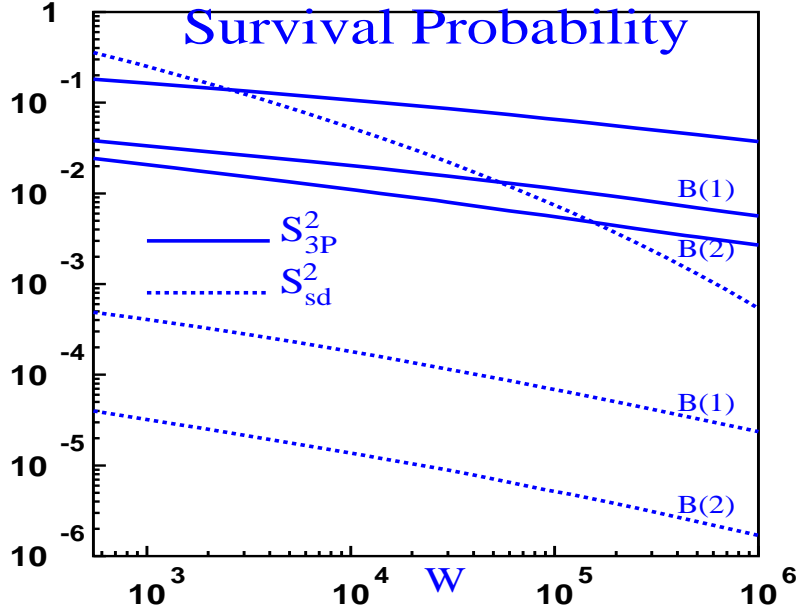


Figure 5: The survival probability for the triple Pomeron vertex in proton-proton collision. S_{3P}^2 denotes the survival probability for the diffraction dissociation in the high mass region (see Eq. (2.21)) , while S_{sd}^2 is the survival probability for the diffractive dissociation in the entire kinematic region (see Eq. (2.28)). The upper curves (full and dotted) refer to model A [?] while the lower curves relate to model B of Ref. [5]

Diffractive processes are also important at cosmic ray energies. Kamae et al [?] have shown that diffractive p-p interactions play a crucial role in understanding the spectrum of galactic gamma-rays that come predominantly from $\pi^0 \rightarrow \gamma\gamma$. The inclusion of diffractive processes makes the gamma ray spectrum harder, and when this is included together with the assumption of Feynman scaling violations, one can explain about 50 per cent of the "GeV Excess". Note, though, that our new diffractive survival probabilities in the Cosmic Ray energy range are exceedingly small.

3. Survival probability for triple Pomeron vertex for J/Ψ -proton collisions.

In this section we calculate the survival probability for high mass diffraction in reaction of Eq. (1.4). From Fig. 2 one can see that we need the following ingredients to make these estimates: the amplitude for the interaction of a colourless dipole with the target, and the description of the J/Ψ production without the additional interaction with the target, which is shown in Fig. 1.

For the scattering dipole amplitude we take a model developed by one of us [?]. This model is based on the solution for a generating functional [?, ?, ?], with an additional assumption: the dipoles do not change

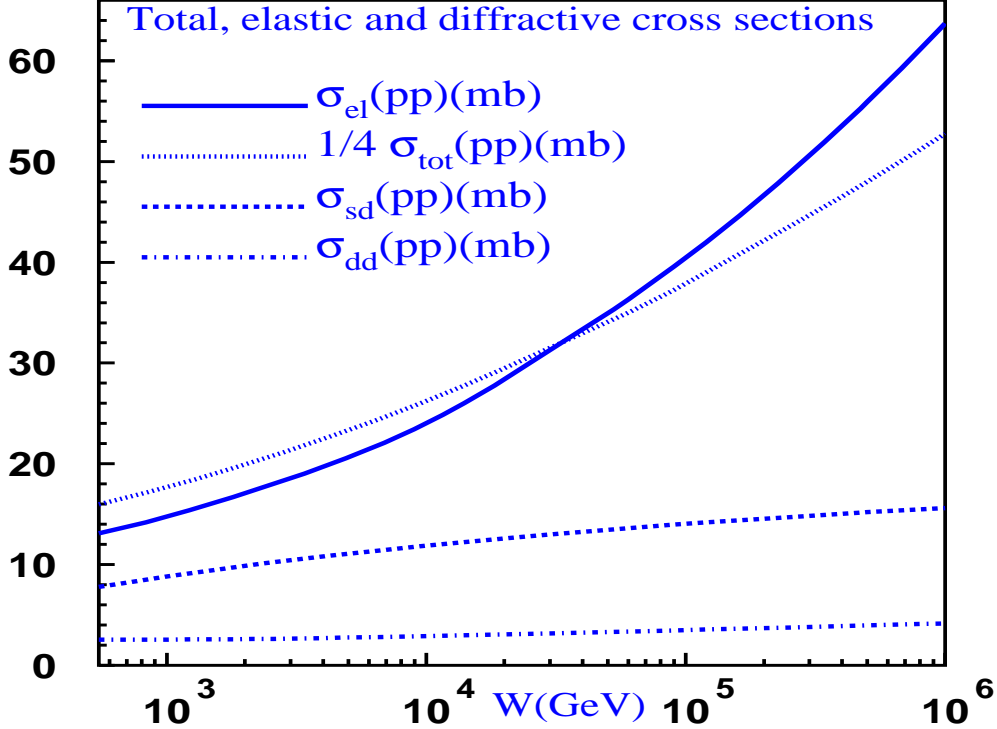


Figure 6: The total, elastic and diffractive dissociation cross sections in model B .

their sizes during the interaction. The amplitude is equal to

$$N(Y = \ln(1/x); r, b) = \frac{\Omega(Y; r, b)}{1 + \Omega(Y; r, b)} \quad (3.1)$$

where

$$\Omega(Y; r, b) = \frac{Q_{s,0}^2 \pi R^2}{4} r^2 x/x_0 G\left(x/x_0, \mu^2 = \frac{C}{r^2} + \mu_0^2\right) S(b); \quad (3.2)$$

$$\text{with } S(b) = \frac{2}{\pi R^2} \frac{\sqrt{8b}}{R} K_1\left(\frac{\sqrt{8b}}{R}\right) \quad (3.3)$$

$$\text{where } Q_{s,0}^2 \text{ is the saturation scale at } x = x_0, Q_{s,0}^2 = Q_s^2(x = x_0) \quad (3.4)$$

The gluon structure function $xG(x, \mu^2)$ satisfies the DGLAP evolution equation with the initial condition $xG(x, \mu_0^2) \propto A/x^{\omega_0}$. In other words, Eq. (3.2) describes the contribution of the hard Pomeron that can be calculated in perturbative QCD. All parameters in Eq. (3.2) have been found by fitting to the data on F_2 . The fit is good and has $\chi^2/d.o.f. = 1.2$ [?]. The values of all the fitted parameters, are close to the

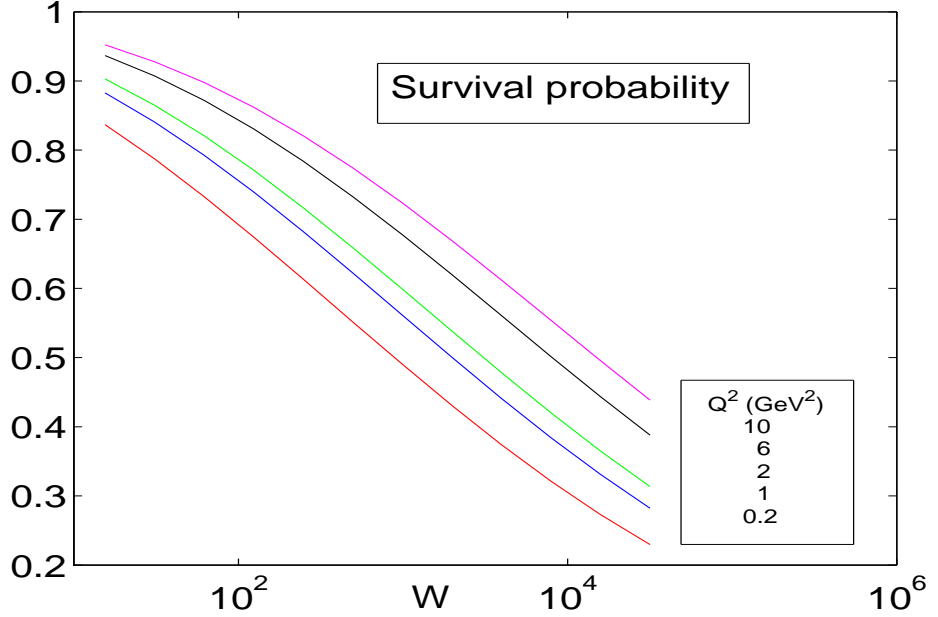


Figure 7: The survival probability for the triple Pomeron vertex in the reaction of Eq. (1.4).

parameter values obtained in other models that are on the market [?]. Eq. (3.3) is the Fourier transform of the electro-magnetic form factor of the proton. Eq. (3.1) is quite different from the eikonal approximation that has been used in all other models, and has a form which is typical for the ‘fan’ diagrams which are summed in the mean field approximation (MFA). One can see directly from Eq. (3.1) and Eq. (3.2) that

$$N(Y = \ln(1/x); r, b) \xrightarrow{r \rightarrow \infty, x \text{ fixed}} 1; \quad N(Y = \ln(1/x); r, b) \xrightarrow{x \rightarrow 0; r \text{ fixed}} 1 \quad (3.5)$$

In Fig. 8 we show how Eq. (3.1) fits the experimental data.

Using Eq. (3.2) we can write the formula for Fig. 1,

$$\begin{aligned} \sigma(\gamma^* + p \rightarrow J/\Psi + M | \text{Fig. 1}) &= G_{3P} (M^2)^{\Delta_P} \int d^2 b \exp\left(-\frac{b^2}{R^2}\right) \\ &\left| \int dz d^2 r \Psi_{\gamma^*}(r, z, Q^2) A(r, x_P) \Psi_{J/\Psi}(r, z) \right| \times \left| \int dz' d^2 r' \Psi_{\gamma^*}(r', z', Q^2) A(r', x_P) \Psi_{J/\Psi}(r', z') \right| \end{aligned} \quad (3.6)$$

where

$$A(r, x_P; b) = \int d^2 b \Omega(Y; r, b) \quad (3.7)$$

In Eq. (3.6) we assume (i) that the hard Pomeron in the upper legs of Fig. 1 does not depend on the impact parameter; and (ii) that the triple Pomeron vertex ($HP - P - HP$) is the same as the triple Pomeron vertex

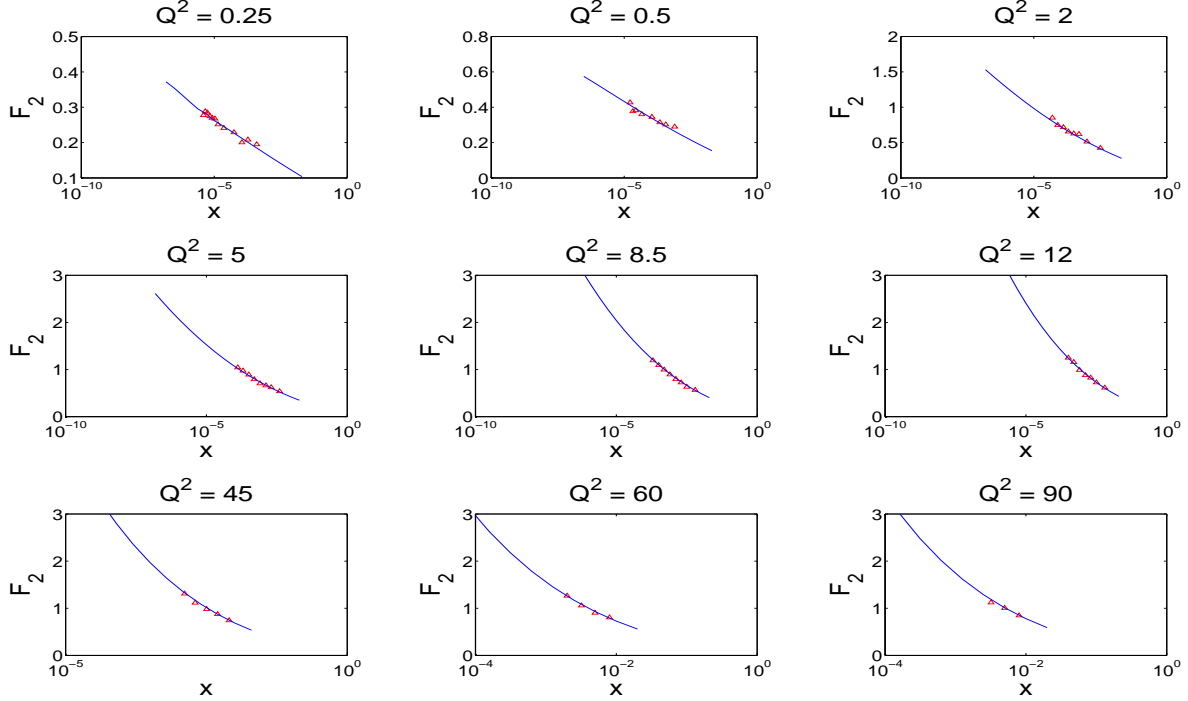


Figure 8: Examples of the fit with Eq. (3.1).

for the soft Pomerons ($P - P - P$) Here, HP denotes the hard Pomeron while P stands for the soft Pomeron. R is the radius for the soft interaction and it was taken to be equal to $R^2 = (12 + \ln(M^2/s_0)) \text{ GeV}^{-2}$ with $s_0 = 1 \text{ GeV}^2$.

The product of wave functions is taken in the form [?]

$$\Psi_{J/\Psi}(r, z = \frac{1}{2}) \times \Psi_{\gamma^*, T}(r; Q^2) = \frac{K_F}{48\alpha_{em}} \sqrt{\frac{3\Gamma_{ee}M_\psi}{\pi}} \times \exp\left(-\frac{r_\perp^2 m_c^2}{3v^2}\right) \times \left\{ \frac{a^2}{m_c} \left(\zeta K_1(\zeta) - \frac{\zeta^2}{4} K_2(\zeta) \right) + m_c \left(\frac{\zeta^2}{2} K_2(\zeta) - \zeta K_1(\zeta) \right) \right\} \quad (3.8)$$

$$\Psi_{J/\Psi}(r, z = \frac{1}{2}) \times \Psi_{\gamma^*, L}(r; Q^2) = \frac{K_F}{48\alpha_{em}} \sqrt{\frac{3\Gamma_{ee}M_\psi}{\pi}} \times \exp\left(-\frac{r_\perp^2 m_c^2}{3v^2}\right) \times \left\{ \frac{Q}{2} \left(\frac{\zeta^2}{2} K_2(\zeta) - \zeta K_1(\zeta) \right) \right\} \quad (3.9)$$

where $\zeta = ar$, Ki , $i = 1, 2$ are the modified Bessel functions, $\Gamma_{ee} = 5.26 \text{ KeV}$ is the leptonic width of the J/Ψ and

$$a^2 = z(1-z)Q^2 + m_c^2 \quad \text{and} \quad x_P = \frac{Q^2 + M^2}{s} \quad (3.10)$$

The exponential factor in Eq. (3.8) and Eq. (3.9) which describes the wave function of J/Ψ meson with velocity v , has been discussed in Ref. [?] and references therein.

For the diagram of Fig. 2 we can write the expression that takes into account the possibility to rescatter before interaction that produces a J/Ψ meson,

$$\begin{aligned} \sigma(\gamma^* + p \rightarrow J/\Psi + M | \text{Fig. 2}) &= G_{3P} (M^2)^{\Delta_P} \int d^2 b \exp\left(-\frac{b^2}{R^2}\right) \quad (3.11) \\ &\left| \int dz d^2 r \Psi_{\gamma^*}(r, z, Q^2) A(r, x_P) (1 - N(Y = \ln(1/x); r, b)) \Psi_{J/\Psi}(r, z) \right| \times \\ &\left| \int dz' d^2 r' \Psi_{\gamma^*}(r', z', Q^2) A(r', x_P) (1 - N(Y = \ln(1/x); r', b)) \Psi_{J/\Psi}(r', z') \right| \end{aligned}$$

The survival probability is the ratio of these two equation (Eq. (3.6) and Eq. (3.11)), namely

$$\langle |S^2| \rangle = \frac{\sigma(\gamma^* + p \rightarrow J/\Psi + M | \text{Fig. 2}; \text{Eq. (3.11)})}{\sigma(\gamma^* + p \rightarrow J/\Psi + M | \text{Fig. 1}; \text{Eq. (3.6)})} \quad (3.12)$$

The results of calculations using Eq. (3.12) are plotted in Fig. 7. One can see that $\langle |S^2| \rangle$ is not close to 1 as was assumed in Ref. [1]. This should be taken into account when attempting to extract the value of the triple Pomeron vertex from the measurement of the cross section of reaction of Eq. (1.4).

4. Conclusions

In this paper we confirm in the context of our two channel model, the wide spread expectation that the survival probability for the triple Pomeron vertex is very small [1, 3, 4]. We also claim that the value of this survival probability is even smaller than the estimates of Ref. [1], which almost coincide with the predictions of our model A. We demonstrated that existing data on double diffraction do not allow us to make a very definite prediction for S_{3P}^2 (see model B predictions in Fig. 5). Therefore, we have to use the experimental data in the region of high masses to specify the parameters of our model.

In this context the data on reaction of Eq. (1.4) are essential, since combining them with the data on the high mass diffraction in proton-proton scattering we are able to get information both on the value of S_{3P}^2 , and the ‘bare’ triple Pomeron vertex.

The survival probability for the reaction of Eq. (1.4) has been calculated, and in spite of the fact that its value turns out to be much smaller than for proton-proton scattering, it cannot be neglected in the analysis aiming to extract the value of the triple Pomeron vertex from the data.

The details of our model B, as well as calculation of the survival probabilities for other large rapidity gaps processes including the diffractive Higgs production in the LHC range of energy, will be published elsewhere.

Acknowledgments:

We are very grateful to Jeremy Miller, Eran Naftali and Alex Prygarin for fruitful discussions on the subject. This research was supported in part by the Israel Science Foundation, founded by the Israeli Academy of Science and Humanities and by BSF grant # 20004019.

References

- [1] V. A. Khoze, A. D. Martin and M. G. Ryskin, “*The extraction of the bare triple-Pomeron vertex: A crucial ingredient for diffraction,*” arXiv:hep-ph/0609312.
- [2] A. B. Kaidalov, V. A. Khoze, Yu. F. Pirogov and N. L. Ter-Isaakyan, Phys. Lett. B **45**, 493 (1973).
- [3] A. B. Kaidalov and K. A. Ter-Martirosyan, “The Pomeron-Particle Total Cross-Section And Diffractive Production Of Nucl. Phys. B **75**, 471 (1974); R. D. Field and G. C. Fox, Nucl. Phys. B **80**, 367 (1974); A. B. Kaidalov, Phys. Rept. **50**, 157 (1979).
- [4] Y. I. Azimov, V. A. Khoze, E. M. Levin and M. G. Ryskin, “Diffraction Dissociation At Modern Energies In The Theory With Sov. J. Nucl. Phys. **23**, 449 (1976) [Yad. Fiz. **23**, 853 (1976)]; “The Processes Of Diffraction Dissociation At Small Momentum Transfer As A Nucl. Phys. B **89**, 508 (1975). V. A. Abramovsky, A. V. Dmitriev and A. A. Schneider, arXiv:hep-ph/0512199; A. Capella, J. Kaplan and J. Tran Thanh Van, “Absorptive Corrections To The Inclusive Spectrum And The Bare Triple Nucl. Phys. B **105**, 333 (1976); V. A. Abramovsky and R. G. Betman, Sov. J. Nucl. Phys. **49**, 747 (1989) [Yad. Fiz. **49**, 1205 (1989)]; K. Goulianos and J. Montanha, Phys. Rev. D **59**, 114017 (1999) [arXiv:hep-ph/9805496]; S. Ostapchenko, Phys. Rev. D **74**, 014026 (2006) [arXiv:hep-ph/0505259]; Phys. Lett. B **636**, 40 (2006) [arXiv:hep-ph/0602139].
- [5] E. Gotsman, E. Levin and U. Maor, Phys. Rev. D **60** (1999) 094011 [arXiv:hep-ph/9902294]; Phys. Lett. B **438** (1998) 229 [arXiv:hep-ph/9804404].
- [6] Yu. L. Dokshitzer, V. Khoze and S.I. Troyan, Proc. “*Physics in Collisions 6*”, p. 417, ed. M. Derrick, WS 1987; Sov. J. Nucl. Phys. **46**, 712 (1987);
Yu. L. Dokshitzer, V. Khoze and T. Sjostrand, Phys. Lett. **B274**, 116 (1992).
- [7] J. D. Bjorken, *Int. J. Mod. Phys. A***7**, 4189 (1992); *Phys. Rev. D***47**, 101 (1993).
- [8] E.A. Kuraev, L.N. Lipatov and V.S. Fadin, Sov. Phys. JETP **45**, 199 (1977) ; Ya.Ya. Balitskii and L.V. Lipatov, Sov. J. Nucl. Phys. **28**, 822 (1978); L.N. Lipatov, Sov. Phys. JETP **63** 904 (1986).
- [9] F. Low, *Phys. Rev. D***12**, 163 (1975); S. Nussinov, *Phys. Rev. Lett.* **34**, 1286 (1975), *Phys. Rev. D***14**, 244 (1976).
- [10] V.A.Khoze, A.D.Martin, M.G.Ryskin, *Phys.Lett. B***401** , 330 (1997); *Phys.Rev. D***56**, 5867 (1997); G. Oderda, G. Sterman, *Phys. Rev. Lett.* **81**, 3591 (1998).
- [11] E. Gotsman, E.M. Levin and U. Maor, *Phys. Lett. B***309**, 199 (1993).
- [12] E. Levin, *Phys. Rev. D***48**, 2097 (1993).
- [13] R.S. Fletcher, *Phys. Rev. D***48**, 5162 (1993).
- [14] A. Rostovtsev and M.G. Ryskin, *Phys. Lett. B***390**, 375 (1997) .

- [15] E. Gotsman, E.M. Levin and U. Maor, *Nucl. Phys.* **B493**, 354 (1997).
- [16] E. Gotsman, E.M. Levin and U. Maor, *Phys. Lett.* **B438**, 229 (1998).
- [17] CDF Collaboration; F. Abe et al., *Phys. Rev. Lett.* **74**, 855 (1995); **80**, 1156 (1998); **81**, 5278 (1998).
- [18] D0 Collaboration, S. Abachi et al., *Phys. Rev. Lett.* **72**, 2332 (1994); *Phys. Rev. Lett.* **76**, 734 (1994); A. Brandt, “*Proceedings of the 4th Workshop on Small-x and Diffractive Physics*”, Sept. 17-20, 1998, FNAL, p.461.
- [19] ZEUS collaboration, M. Derrick et al., *Phys. Lett.* **B315**, 481 (1993); *Z. Phys.* **C68**, 569 (1995); *Phys. Lett.* **B369**, 55 (1996).
- [20] E.L. Feinberg, *ZhETP* **29**, 115 (1955); A. I. Akieser and A.G. Sitenko, *ZhETP* **32**, 744 (1957).
- [21] M.L. Good and W.D. Walker, *Phys. Rev.* **120**, 1857 (1960).
- [22] J. Pumplin, *Phys. Rev.* **D8**, 2899 (1973).
- [23] A. Donnachie and P.V. Landshoff, *Nucl. Phys.* **B244**, 322 (1984); *Nucl. Phys.* **B267**, 690 (1986), *Phys. Lett.* **B296**, 227 (1992); *Z. Phys.* **C61**, 139 (1994).
- [24] L.V. Gribov, E.M. Levin and M.G. Ryskin, *Phys. Rep.* **100**, 1 (1983).
- [25] E. Gotsman, E. Levin and U. Maor, *Phys. Lett.* **B425**, 369 (1998); E. Gotsman, E. Levin, U. Maor and E. Naftali, DESY 98-102, TAUP 2515/98, [hep-ph/9808257](#), *Nucl. Phys.* **B** (in press).
- [26] F. Abe et al., CDF Collaboration, FERMILAB-PUB-97/083-E.
- [27] K.G. Boreskov, A. M. Lapidus, S.T. Sukhorukov and K.A. Ter-Martirosyan, *Nucl. Phys.* **B40**, 397 (1972); P.E. Volkovitsky and A.M. Lapidus, *Sov. J. Nucl. Phys.* **31**, 380 (1980).
- [28] K. Goulianos, *Phys. Rep.* **C101**, 169 (1983).
- [29] E. Gotsman, E. Levin and U. Maor, TAUP 2560 - 99, [hep-ph/9901416](#).
- [30] S. Aid et al., H1 Collaboration, *Nucl. Phys.* **B472**, 3 (1996); M. Derrick et al., ZEUS Collaboration, *Phys. Lett.* **B350**, 120 (1996).

$S^2(W)$

